

# Numerical simulation of collaboratively designed flow channel and gas diffusion layer structures for proton exchange membrane fuel cell

Xiaojian Zhang<sup>1</sup>, Jiaojiao Song<sup>1</sup>, Chao Guan<sup>1</sup>, Yulin Wang<sup>1,2,3\*</sup>

<sup>1</sup> Tianjin Key Lab of Refrigeration Technology, Tianjin University of Commerce, Tianjin 300134, China.

<sup>2</sup> Key Laboratory of Advanced Fuel Cells and Electrolyzers Technology of Zhejiang Province, Ningbo 315200, China;

<sup>3</sup> Ningbo Institute of Material Technology and Engineering, Chinese Academy of Sciences, Ningbo 315200, China

(Corresponding Author: [wangylfcs@gmail.com](mailto:wangylfcs@gmail.com))

## ABSTRACT

For hydrogen polymer electrolyte membrane fuel cell (PEMFC), the structure design of the bipolar plate (BP) and gas diffusion layer (GDL) greatly affects the water and gas transport and the performance of the PEMFC. Starting with the length and cross-section size of the flow channel (FCH), the thickness of the GDL, the average porosity and the degree of porosity gradient in the flow direction, this paper studies the effect of the collaborative matching optimization of the BP and GDL structure on the performance of the PEMFC. Firstly, five variables including average porosity, GDL thickness, porosity gradient degree, FCH cross-section and length are selected as matching factors (five-level numbers for each variable), and two performance parameters including maximum power density and pressure drop are used as performance evaluation indexes. Secondly, the orthogonal table is established by orthogonal experimental design. The range analysis and variance analysis are carried out on the Orthogonal test results after the data is obtained through simulation. Finally, the Entropy weighting method is used to evaluate the two performance evaluation indexes of 26 groups of data. The results show that Case 18 has the highest comprehensive evaluation index, with an evaluation index of 0.06055 and the base group is 0.04655. Compared to the base case, the maximum power density of case 18 is increased by 19.8%.

**Keywords:** Bipolar plate, Gas diffusion layer, orthogonal experimental, Entropy weighting method, Cell performance.

## NOMENCLATURE

### Abbreviations

PEMFC	polymer electrolyte membrane fuel cell
FCH	flow channel
GDL	gas diffusion layer
PTFE	polytetrafluoroethylene
PEM	polymer electrolyte membrane
CL	catalyst layer
BP	bipolar plate

### Symbols

$a$	anode
$c$	cathode
$r$	reaction
ref	reference
$F$	faraday coefficient
$R$	universal gas constant
$T$	temperature
$A$	area
$i$	current density
$P$	pressure
sat	saturation
$\xi$	inlet gas stoichiometric ratio

## 1. INTRODUCTION

Proton exchange membrane fuel cell (PEMFC) is a clean energy conversion device that directly converts the chemical energy in hydrogen and oxygen into electrical energy. It has the characteristics of high energy conversion efficiency, low pollutant emission, fast start-up speed, high reliability and strong flexibility, which is considered to be one of the best solutions to environmental pollution and energy crisis [1-3]. However, there are still some key problems to realize the commercialization of PEMFC, such as revealing the

multi-field coupling transmission mechanism of water, gas, electricity and heat inside the PEMFC, developing new PEMFC materials to reduce production costs and designing structures for membrane electrodes and bipolar plates (BP), to improve the overall output performance of PEMFC, extend service life and reduce costs.

The flow field structure of the BP determines the flow state of the reaction gas and the product in the flow field and the long-term stability of the PEMFC. A well-designed flow field is essential in effectively distributing the reaction gas required for the PEMFC and ensuring an even distribution of current density. At the same time, it can timely and smoothly discharge the water generated by the PEMFC with the flow channel (FCH), ensuring the stable performance of the PEMFC [4,5]. Thus far, various flow field structures have been developed for PEMFC, including traditional designs such as parallel, interdigitated, and serpentine flow fields [6], as well as newer designs such as bionic, ring, radial, and mixed flow fields [7,8]. Numerous studies claim that a good flow field design can improve the utilization rate of reactant gas, improve the removal capacity of liquid water, and thus improve the overall performance of the PEMFC.

The gas diffusion layer (GDL) is one of the important components of PEMFC. It is a complex porous medium structure. It is responsible for the diffusion of gas and the transport of liquid water. Reasonable design of the diffusion layer structure is conducive to improving the gas diffusion and liquid water drainage inside the PEMFC, which can contribute to the improvement of PEMFC performance. The design of the GDL includes the optimization of the content and distribution of the polytetrafluoroethylene (PTFE) [9] and the GDL thickness, pore size and distribution [10,11]. At the same time, it should be noted that the porosity of the GDL will not only affect the diffusion coefficient and permeability but also affect the conductivity of the GDL.

In recent years, most researchers have studied the structure of BP and GDL separately. Either studied the effect of BP structure optimization on the drainage capacity and PEMFC performance, or studied the effect of GDL structure on the mass transfer performance and PEMFC performance. Our paper studies the influence of the synergistic effect of the matching structure of BP

and GDL on the PEMFC performance, which explores the correlation between five variables (cross-section size and length of the FCH, the average porosity and thickness of the GDL and the gradient distribution of porosity along the flow direction) and the PEMFC output performance. The effects of different combinations on maximum power density and pressure drop are observed. Meanwhile, in order to reduce the experience burden, we carry out an orthogonal test design and analyze the orthogonal test results to get the relationship between factors and performance indicators. Finally, overall output performances of PEMFC are comprehensively evaluated with the entropy weight method.

## **2. MATHEMATICS MODEL**

### *2.1. Model computational domain*

The PEMFC is made up of BP, GDL, catalyst layer (CL) and the proton exchange membrane (PEM). In addition to PEM, the other components are divided into cathode and anode. Cross-section size of FCH (ranging from  $0.6 \times 0.6$  to  $1.4 \times 1.4$  mm<sup>2</sup>) and length (ranging from 60 to 140 mm), GDL thickness (ranging from 0.1 to 0.3 mm), GDL average porosity (ranging from 0.4 to 0.8) and gradient distribution in the direction of the FCH has five gradients. The thickness of the anode and of the cathode CL is 0.01 mm, and the thickness of the PEM is 0.025 mm. Due to the symmetry of the parallel flow field, the model is calculated in the form of half-FCH and half-rib. The reactive area changes with the CH size.

### *2.2 Model assumptions and governing equations*

The model assumes that the fuel cell operates under non-isothermal, polyphase, and steady-state conditions. Incompressible fluid laminar flow; The reaction gas is ideal. The thermal conductivity of porous electrodes such as PEM, CLs and GDLs is isotropic. Water in PEM is in the dissolved phase; The simulation also takes into account the phase transition between vapor water, liquid water and dissolved water.

The PEMFC model includes partial differential conservation equations of mass, momentum, matter, liquid water transport, dissolved water transport, electron proton transport and energy. The mathematical descriptions and corresponding source terms are presented in our previous work [3]. In

addition, the Butler-Volmer equation is also used to deal with the electrochemical solution of current density in the CL which involves charge transfer and energy conservation equations. The Leverett J function and Wyllie model are used to describe liquid water transport in GDL and CLs. Additionally, the transport and input parameters of the model are mentioned in our previous work [3].

### 2.3. Boundary conditions

It is assumed that the wall temperature of the PEMFC is fixed at 80°C and operates at 1 atm without a sliding wall. The inlet is set as the mass flow inlet and the outlet as the pressure outlet. The anode is fixed at 0 v potential, and the cathode is Operating Voltage. The mass flow rate, which is determined by

$$m_a = \frac{\rho_a \xi_a i_{ref} A_r}{2F} \frac{RT}{p_a - RH_a p^{sat}}, m_c = \frac{\rho_c \xi_c i_{ref} A_r}{4F} \frac{RT}{0.21(p_c - RH_c p^{sat})}, \text{ here } \rho_a$$

and  $\rho_c$  are the anode and cathode gas mixture densities,  $\xi_a$  and  $\xi_c$  are the anode and cathode inlet gas stoichiometric ratio,  $i_{ref}$  is the reference current density,  $A_r$  represents the area of the reaction site,  $p_a$  and  $p_c$  are the inlet pressure of the anode and cathode FCH,  $RH_a$  and  $RH_c$  are the relative humidity of the anode and cathode inlet gas, and  $p^{sat}$  is the water vapor saturation pressure.

### 2.4. Numerical implementation and model validation

Continuity, momentum, species and energy equations in the PEMFC model are solved by Ansys fluent 19.2. In addition, four user-defined scalar (UDS) conservation equations are compiled in C code by means of user-defined functions (UDF) to solve conservation equations. In the process of solving, the SIMPLE algorithm is used to deal with the velocity and pressure coupling in the momentum equation, the UDS equation adopts the second-order upwind format, and the other terms are the first-order upwind format, and the double-precision model is solved.

To validate the PEMFC model developed here, grid independence tests are performed between three different grid sizes with total elements of 232800, 362660, and 533800. The simulation results show that the relative deviation of the current density of three different mesh sizes is less than 1.5% under the same operating voltage. In addition, the predicted polarization curves are compared with published

experimental data and numerical results when the integral number of ionomer objects in CL is 0.22 and 0.27 in Fig 1.

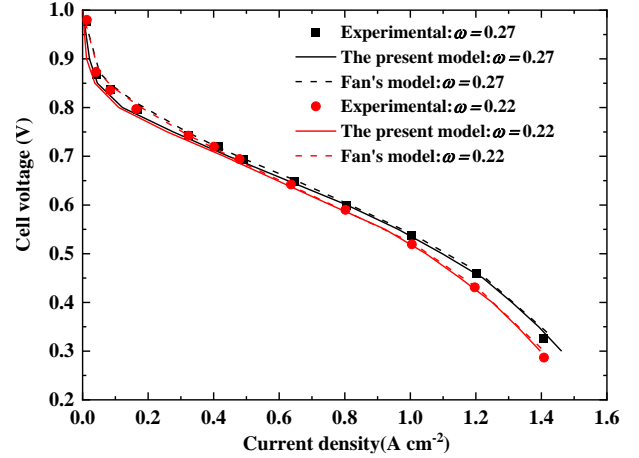


Fig 1 Comparison of polarization curves with the experimental and numerical results

## 3. RESULT AND DISCUSSION

### 3.1 Selection of structure parameter and Orthogonal table

The structure of the conventional parallel flow field is mainly manifested in the width ratio of the FCH to the rib and the length of the FCH. In this paper, the length and width of the inlet section of the FCH are consistent, but the cross-section size and length of the FCH are changed. The structure of GDL is mainly manifested in its thickness and porosity size, and our previous work found that the porosity distribution on GDL will also affect the overall performance of the PEMFC [3], so it is necessary to add the variable of porosity gradient (Fig 2).

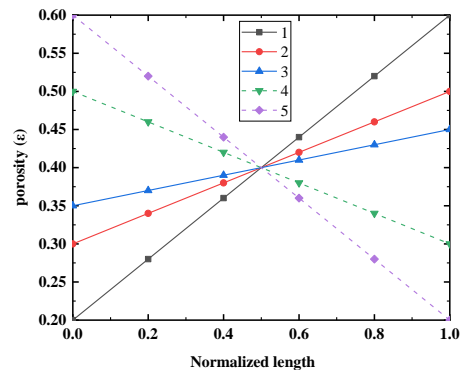


Fig 2 Five designs of gradient porosity for GDL with an average porosity of 0.4

Since five variables are considered at the same time and each variable has five levels, if all of these are combined, there are 3,125 combinations. It is obviously unrealistic to simulate all groups, so we add orthogonal tables. The orthogonal table has the characteristics of

orthogonality, balanced distribution of points in space, uniform dispersion, and neat comparability of data arranged in the table, which can accurately evaluate the influence of single factors on the results. The advantage of an orthogonal table is that it can analyze Partial experiments instead of all experiments, which greatly saves the cost of experiments. The orthogonal experiment design of five factors and five levels is carried out to obtain an orthogonal table containing 25 groups, and 25 groups of partial experiments are used to replace all the experiments of 3125 groups. It is shown In Table 1 The experimental results are supplemented by simulation.

**Table 1**

*Orthogonal table (base not included)*

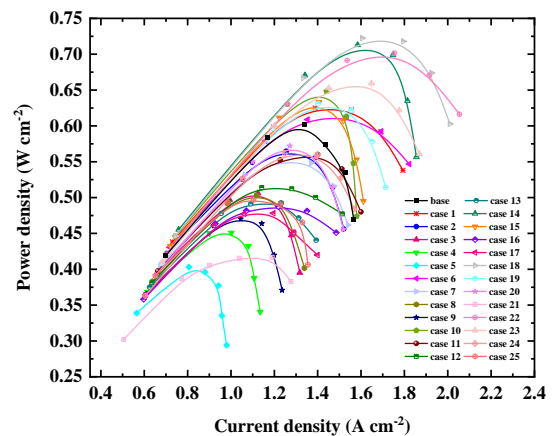
Number	Average Porosity	Width of GDL	Size of channel	Size of gradient	Length
base	0.7	300	1×1	0	100
1	0.4	100	0.6×0.6	1	60
2	0.4	150	0.8×0.8	2	80
3	0.4	200	1×1	3	100
4	0.4	250	1.2×1.2	4	120
5	0.4	300	1.4×1.4	5	140
6	0.5	100	0.8×0.8	3	120
7	0.5	150	1×1	4	140
8	0.5	200	1.2×1.2	5	60
9	0.5	250	1.4×1.4	1	80
10	0.5	300	0.6×0.6	2	100
11	0.6	100	1×1	5	80
12	0.6	150	1.2×1.2	1	100
13	0.6	200	1.4×1.4	2	120
14	0.6	250	0.6×0.6	3	140
15	0.6	300	0.8×0.8	4	60
16	0.7	100	1.2×1.2	2	140
17	0.7	150	1.4×1.4	3	60
18	0.7	200	0.6×0.6	4	80
19	0.7	250	0.8×0.8	5	100
20	0.7	300	1×1	1	120
21	0.8	100	1.4×1.4	4	100
22	0.8	150	0.6×0.6	5	120
23	0.8	200	0.8×0.8	1	140
24	0.8	250	1×1	2	60
25	0.8	300	1.2×1.2	3	80

### 3.2 Analysis of orthogonal experimental result

Range analysis, also known as intuitive analysis, is the most commonly used analysis method for orthogonal experimental analysis because of its simple and intuitive data processing. By calculating the mean of each group of levels, the relationship between different levels and performance indicators is obtained, and the difference between the maximum and minimum values of the mean is used to describe the degree of data dispersion and determine the degree of influence of the factor on the performance indicators. As a statistical test method, analysis of variance (ANOVA) can be used to test the significance of the influence of relevant factors on the test results during the test process. In the analysis, blank columns are added to consider the data fluctuations caused by random errors in the process, and the results of ANOVA are more accurate than those of range analysis. The orthogonal test results are analyzed by range analysis and ANOVA, and Polarization curves, power density curves, which is show in Fig 3.

For power density, FCH cross-section is the most significant factor, porosity and GDL thickness are the most significant factors, and gradient degree and length have the least influence. In terms of the FCH cross-section, the smaller the size of the FCH cross-section, the greater the corresponding power density value and the better the performance.

For the pressure drop, the FCH cross-section is also the most significant factor, while FCH length has no significant effect on the pressure drop, but it has a greater impact than the other three factors, and the other factors have little impact. In terms of the cross-section of the FCH, the larger the size of the FCH cross-section, the smaller the pressure drop.



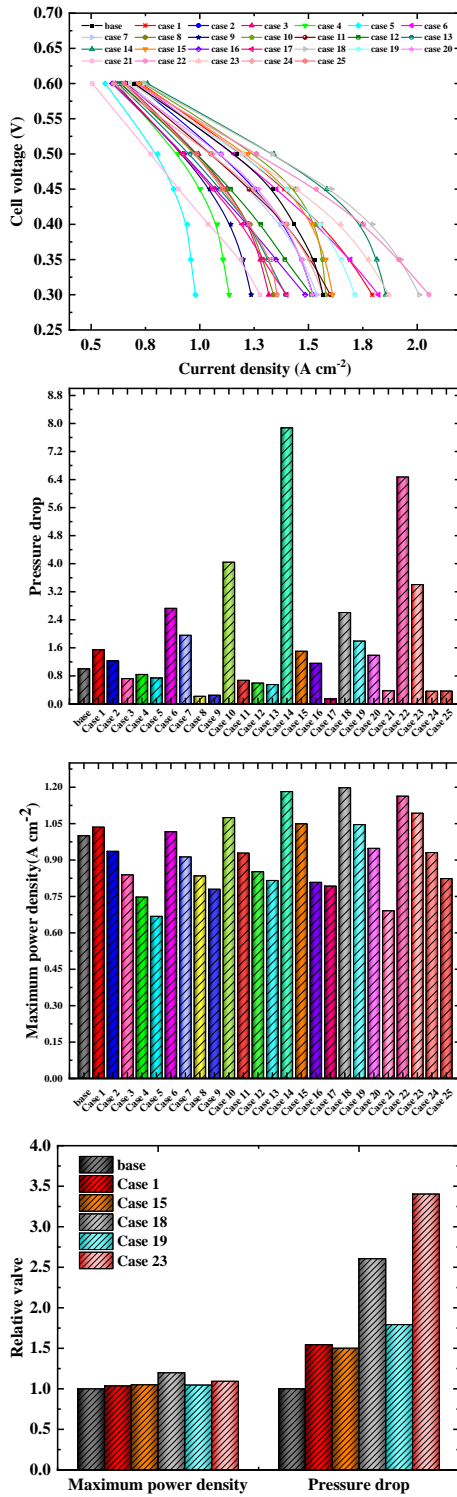


Fig 3 Polarization curves, power density curves and bar graph of power density and pressure drop

### 3.3 Entropy weight analysis

The entropy weight method is used to optimize 26 groups of data with two objectives, power density and pressure drop, and a comprehensive evaluation is carried out. According to the entropy weight analysis in Table 2, the weight coefficients of maximum power density and pressure drop are 0.614 and 0.386 respectively, which shows that the information entropy

contained in power density is greater than pressure drop from a statistical point of view, and also indicates that the importance of maximum power density is greater than pressure drop in comprehensive evaluation. The bar chart shows the six groups of data with high comprehensive evaluation values. It can be seen from the bar chart that Case 18 has the highest power density and the fifth highest pressure drop, while the highest comprehensive evaluation value is 0.06104 for Case 18 and 0.0466 for base. Compared with the base, the maximum power density of Case 18 has increased by 19.8%.

**Table 2**

*Comprehensive evaluation value of 26 sets of data*

Number	Maximum power density	Pressure	Evaluation index
base	0.6033	169.71	0.0466
1	0.6249	262.05	0.0485
2	0.5646	207.80	0.0402
3	0.5061	122.12	0.0327
4	0.4509	142.61	0.0241
5	0.4030	125.10	0.0172
6	0.6132	462.58	0.0439
7	0.5506	332.18	0.0364
8	0.5036	36.83	0.0335
9	0.4703	42.01	0.0284
10	0.6482	686.11	0.0460
11	0.5602	114.09	0.0409
12	0.5139	100.82	0.0342
13	0.4921	93.75	0.0310
14	0.7130	1336.51	0.0464
15	0.6329	254.72	0.0498
16	0.4874	196.46	0.0288
17	0.4782	23.83	0.0299
18	0.7225	442.18	0.0605
19	0.6310	304.16	0.0488
20	0.5720	235.29	0.0409
21	0.4166	63.51	0.0201
22	0.7016	1098.32	0.0481
23	0.6594	577.69	0.0492
24	0.5616	61.35	0.0419
25	0.4968	62.33	0.0321

### 4. CONCLUSION

The variance analysis shows that the significant influence factor of the maximum power density and pressure drop is the FCH cross-section. The analysis of the range shows that if the cross-section size of the FCH is smaller, the power density will be greater. When the cross-section of the FCH is larger, it has a smaller pressure drop.

The weight coefficients of the maximum power density and of the pressure drop are 0.614 and 0.386

respectively. Among them, the highest evaluation value of Case 18 is 0.6055, and its corresponding parameters are porosity 0.7, GDL thickness 200  $\mu\text{m}$ , FCH cross-section  $0.6 \times 0.6 \text{ mm}^2$ , gradient degree 1, and FCH length 80 mm. Case 5 has the lowest rating of 0.01719.

#### ACKNOWLEDGMENT

The authors are grateful for the financial support from the National Key Research and Development Program of China (No. 2022YFE0207600), the Tianjin Natural Science Foundation for Outstanding Young Scholar (No.23JCJQJC00290), the National Natural Science Foundation of China (No. 52176084), YongJiang Talent Engineering Technology Innovation Team Project of Zhejiang province, China (NO.2022A-008-C) and Project of State Key Laboratory of Intelligent Green Vehicle and Mobility (No. KFY2403).

#### DECLARATION OF INTEREST STATEMENT

The authors declare that they have no known competing financial interests or personal relationships that could have appeared to influence the work reported in this paper. All authors read and approved the final manuscript.

#### REFERENCE

[1] Chen G Y, Wang C, Lei Y J, Zhang J, Mao Z, Mao Z Q, et al. Gradient design of Pt/C ratio and Nafion content in cathode catalyst layer of PEMFCs. *International Journal of Hydrogen Energy*, 2017, 42(50): 29960-65.

[2] Mohammedi A, Sahli Y, Moussa HB. 3D investigation of the channel cross-section configuration effect on the power delivered by PEMFCs with straight channels. *Fuel* 2020, 263: 116713.

[3] Wang Y, Wang X, Qin Y, Zhang L, Wang Y. Three-dimensional numerical study of a cathode gas diffusion layer with a through/in plane synergetic gradient

porosity distribution for PEM fuel cells. *International Journal of Heat and Mass Transfer*, 2022, 188: 122661.

[4] Fan L, Niu Z, Zhang G, Jiao K. Optimization design of the cathode flow channel for proton exchange membrane fuel cells. *Energy Convers Manag.* 2018, 171:1813–21.

[5] Wang Y, Xu H, Wang X, Gao Y, Su X, Qin Y, et al. Multi-sub-inlets at cathode flow-field plate for current density homogenization and enhancement of PEM fuel cells in low relative humidity. *Energy Convers Manag.* 2022, 252: 115069.

[6] Marappan M, Palaniswamy K, Velumani T, Chul K B, Velayutham R, Shivakumar P, et al. Performance studies of proton exchange membrane fuel cells with different flow field designs—review. *The Chemical Record*, 2021, 21(4): 663-714.

[7] Kloess J P, Wang X, Liu J, Shi Z, Guessous L. Investigation of bio-inspired flow channel designs for bipolar plates in proton exchange membrane fuel cells. *Journal of Power Sources*, 2009, 188(1): 132-140.

[8] Zhang S, Xu H, Qu Z, Liu S, Talkhonchek F K. Bio-inspired flow channel designs for proton exchange membrane fuel cells: A review. *Journal of Power Sources*, 2022, 522: 231003.

[9] Yue L, Wang S, Araki T, Utaka Y, Wang Y. Effect of water distribution in gas diffusion layer on proton exchange membrane fuel cell performance. *International Journal of Hydrogen Energy*, 2021, 46(3): 2969-77.

[10] Kanchan B K, Randive P, Pati S. Numerical investigation of multi-layered porosity in the gas diffusion layer on the performance of a PEM fuel cell. *International Journal of Hydrogen Energy*, 2020, 45(41): 21836-21847.

[11] Ko D, Doh S, Park H S, Kim M H. The effect of through plane pore gradient GDL on the water distribution of PEMFC. *International Journal of Hydrogen Energy*, 2018, 43(4): 2369-2380.